

## DOPPLERONS IN CADMIUM

L. M. FISHER, V. V. LAVROVA, V. A. YUDIN, O. V. KONSTANTINOV, and V. G. SKOBOV

All-Union Electrotechnical Institute; A. F. Ioffe Physicotechnical Institute,  
USSR Academy of Sciences

Submitted August 10, 1970

Zh. Eksp. Teor. Fiz. 60, 759-774 (February, 1971)

Oscillations of surface impedance of single-crystal plates of cadmium in a magnetic field normal to the surface and parallel to the hexagonal axis were observed experimentally and investigated theoretically. At a frequency of 1 MHz, the oscillations exist in the interval from 7.5 to 13.5 kOe. With increasing frequency, the boundary fields increase in proportion to the cube root of the frequency. The period of the oscillation increases with the field, changing by 30-50%. Near the upper boundary, the period reaches a limiting value that depends only on the thickness of the plate. These oscillations are connected with excitation of an electromagnetic wave ("doppleron") due to the Doppler-shifted cyclotron resonance of the lens electrons. A theoretical analysis shows that near the upper boundary, the doppleron oscillations go over into oscillations of the Gantmakher-Kaner size effect. Measurement of the period of the oscillations has made it possible to determine the radius of curvature of the lens at the limiting point  $k_F = 1.49 \pm 0.08 \text{ \AA}^{-1}$ . The experimental boundaries of the region of existence of the doppleron and the change of the period are in good agreement with the theoretical values obtained from the free-electron model.

## 1. INTRODUCTION

WE have observed experimentally and investigated theoretically electromagnetic waves capable of propagating in cadmium in a magnetic field normal to the surface of the sample. The range of frequencies and magnetic fields for these waves coincides approximately with the region of the Doppler-shifted cyclotron resonances of helicons in uncompensated metals. This circumstance is not accidental, since the physical nature of both these phenomena is the same—Doppler-shifted cyclotron resonance of definite groups of electrons on the Fermi surface. In alkali metals, the propagation of helicons occurs only in sufficiently strong magnetic fields, when the displacement of the electron along the field during the cyclotron period is smaller than the wavelength of the helicon. With decreasing field, these quantities come closer together, and when the maximum displacement over the period (for electrons traveling opposite to the wave) turns out to be equal to the helicon wavelength, a collisionless cyclotron absorption sets in and makes wave propagation impossible. This absorption threshold corresponds to equality of the cyclotron frequency to the Doppler shift of the frequency of the wave in a coordinate system moving together with the electrons of the limiting point. The nonlocal conductivity of the degenerate electron gas has a singularity in this case. The character of the singularity depends strongly on the law of dispersion of that group of electrons which is responsible for the Doppler-shifted cyclotron resonance. In alkali metals this resonance is due to the electrons of the limiting point, which lead to a singularity of the type  $x \ln x$  in the imaginary part of the nonlocal conductivity.

Chambers and Skobov<sup>[1]</sup> and Falk, Gerson, and Carolan<sup>[2]</sup> considered models of anisotropic Fermi surfaces, which give stronger singularities of the nonlocal conductivity, and have shown that such singularities lead to the occurrence of new types of electromag-

netic waves in metals. The main property of these waves is that their length is quite close to the average displacement of the electrons during the cyclotron period. The presence of such a mode of the electromagnetic spectrum was in essence first indicated by McGroddy, Stanford, and Stern<sup>[3]</sup> and by Overhauser and Rodriguez,<sup>[4]</sup> who investigated the edge of the cyclotron absorption in alkali metals. In<sup>[5]</sup> it was shown that the wave due to the Doppler-shifted cyclotron resonance can also propagate in alkali metals in another geometry, when the magnetic field is directed at a small angle to the surface of the sample. It is natural to call this entire aggregate of waves dopplérons, since their dispersion law reflects almost exactly the equality of the cyclotron frequency to the Doppler-shifted frequency of the wave in a coordinate system moving together with the characteristic group of electrons.

The present paper is devoted to an investigation of dopplérons in cadmium, in which the concentrations of the electrons and the holes are equal and the propagation of helicons is impossible. In the third energy band of cadmium, and also of zinc and magnesium, there is an electronic Fermi surface having the form of a lens.<sup>[6]</sup> The velocities of the lens electrons are large and lie in a narrow interval, so that these electrons form two opposing beams. Other groups of carriers apparently have much lower velocities, and therefore a situation is possible wherein the nonlocal effects are strong for the conductivity of the lens electrons and weak for the conductivity of the remaining carriers. To this end it is required that the average displacement of the electrons of the lens along the magnetic field directed parallel to the hexagonal axis be close to the wavelength of the doppleron, and the displacements of the remaining carriers be much smaller than the wavelength. In other words, the Doppler-shifted frequency of the wave in a system moving with the electrons of the limiting point of the lens will be close to the cyclotron frequency. For other groups of carriers, the Doppler frequency shift

will be smaller. Under these conditions, the nonlocal Hall conductivity of the lens electrons turns out to be much larger than its local limit and is not compensated by the contribution of the remaining carriers, as is the case at large wavelengths. This makes it possible for the doppleron to propagate.

A doppleron propagating along the magnetic field has circular polarization. The direction of rotation of the electric vector of the wave coincides with the direction of rotation of the electrons, in analogy with the helicon.

The propagation of a Doppleron in a plate of finite thickness is accompanied by interference oscillations of the impedance as a function of the magnetic field, in analogy with the situation for helicons. As already mentioned above, the wavelength of the doppleron is close to the displacement of the electrons of the limiting point during the cyclotron period. Therefore the transition from one interference maximum to another corresponds to a unity change in the number of displacements subtended by the sample. From this point of view, the doppleron oscillations are quite similar to the oscillations of the Gantmakher-Kaner radio-frequency size effect.<sup>[7]</sup> It is shown in the present paper that in cadmium the regions of magnetic fields in which the doppleron and the Gantmakher-Kaner wave exist lie alongside each other and even overlap somewhat. The doppleron exists in weaker magnetic fields, and its amplitude greatly exceeds the amplitude of the radio-frequency size effect, while the period of the oscillations is smaller than the period of the size effect. In strong fields, the amplitude of the doppleron decreases and the period of the oscillations increases, so that a continuous transition takes place to Gantmakher-Kaner oscillations, a distinguishing feature of which is constancy of the period.

## 2. MEASUREMENT PROCEDURE

We investigated the surface resistance of single-crystal plates of cadmium in a magnetic field normal to the surface of the sample. We measured the dependence of the derivative of the surface resistance on the magnetic field in the frequency range 0.8–8 MHz. Plane-parallel cadmium samples were cut by the electric spark method from a single crystal, and were etched after cutting in concentrated hydrochloric acid. We investigated plates with dimensions  $12 \times 4$  mm and with thicknesses 0.40, 0.76, 1.46, and 1.48 mm. The resistance ratio was  $\rho(300^\circ\text{K})/\rho(4.2^\circ\text{K}) = (10-12) \times 10^3$ . The orientation of the samples was determined by x-ray diffraction. The normal to the plate coincided with the direction of the hexagonal axis [0001], and the major axis of the sample was parallel to the [11 $\bar{2}$ 0] direction.

The measurements were performed with a setup similar to a spectrometer for the observation of NMR. The block diagram of the setup is shown in Fig. 1.

The small-amplitude generator was a tapped-capacitor oscillator. The use of negative feedback made it possible to stabilize the amplitude of the oscillations and the operating conditions of the generator. As a result, it was possible to carry out amplitude measurements of the  $dR/dH = f(H)$  of samples in a magnetic field, when the  $Q$  of the tank circuit changes strongly. When the  $Q$  changed by a factor of 5, the error in the

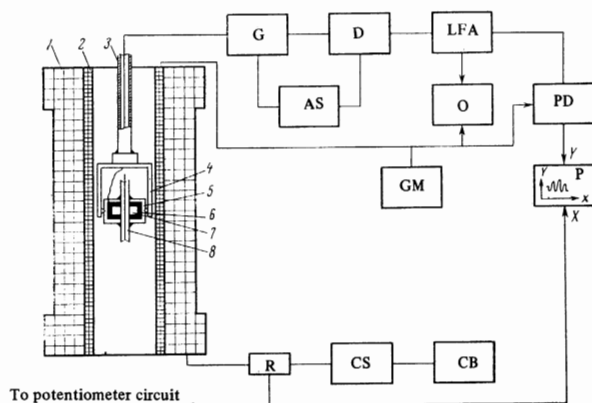


FIG. 1. Block diagram of measuring setup: 1—superconducting solenoid, 2—modulation coil, 3—coaxial cable, 4—fork, 5—sample holder, 6—high-frequency coil, 7—sample, 8—cord-driven pulley, G—small-amplitude generator, D—detector, AS—amplitude stabilization system, LFA—low-frequency amplifier, O—oscilloscope, PD—phase detector, GM—modulation generator, P—x-y plotter, R—standard resistance, CS—current stabilizer, CB—control block.

measurement of the amplitude was  $\sim 1\%$ . The stabilization system had a large time constant (on the order of 10 seconds), so that it exerted no influence on the signal at the modulation frequency (10 Hz). This system will be described in detail in a separate article.

The sample was placed in a flat induction coil of the tank circuit of the generator. The coil was mounted on a polystyrene holder and was immersed in liquid helium. Three interchangeable coils with three or four layers of turns were used to cover the frequency band 0.8–10 MHz.

The magnetic field was produced with the aid of a superconducting solenoid with a maximum field 50 kOe. The diameter of the solenoid channel was 24 mm and the height was 100 mm. The magnetic field  $H$  was determined from the current  $I$  flowing through the solenoid:  $H = \kappa_0 I$ . The solenoid constant  $\kappa_0$  was determined from signals of nuclear magnetic resonance on protons in weak fields ( $H \lesssim 2$  kOe) and on aluminum and copper ( $\text{Cu}^{63}$  and  $\text{Cu}^{65}$ ) nuclei in fields  $\sim 10$  kOe. In this field interval,  $\kappa_0$  was independent of the magnetic field and amounted to 1.885 kOe/A. The current  $I$  was measured with a potentiometer circuit and determined from the voltage drop across a standard resistance.

The constant magnetic field was modulated at low frequency (10 Hz) with amplitude up to 300 Oe. The alternating field was produced by an additional superconducting coil fed from a low-frequency generator.

The orientation of the samples in the magnetic field was varied with the aid of a rotating device. The sample together with the coil could be rotated about the horizontal axis through  $360^\circ$ . The rotation angle was controlled accurate to  $1^\circ$  by means of a micrometer screw coupled to a drive cord, the other end of which was fastened to a spring. The orientation at which the field was normal to the surface of the sample was determined approximately from the minimum induced modulated signal in the inductance coil of the tank circuit. This orientation was determined more accurately from the symmetry of the  $dR/dH = f(\theta)$  curves ( $\theta$  is the angle between the normal to the sample and the magnetic field).

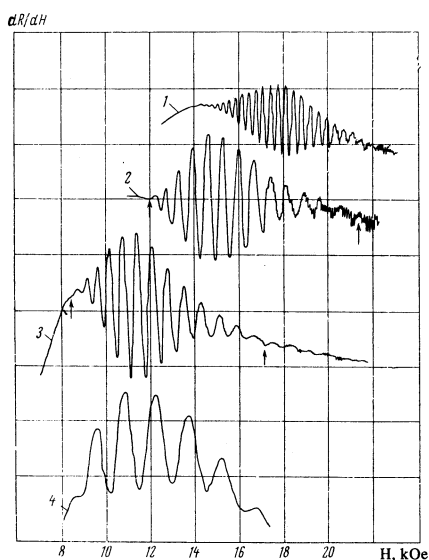


FIG. 2. Plots of the derivative of the surface resistance. Curve 1—sample III,  $d = 1.46$  mm,  $f = 5.7$  MHz; 2—sample II,  $d = 0.76$  mm,  $f = 4.06$  MHz; 3—sample II,  $f = 1.67$  MHz; 4—sample I,  $d = 0.4$  mm,  $f = 1.60$  MHz.

A signal proportional to  $dR/dH$  was fed to the Y coordinate of the automatic potentiometer PDS-021; the X coordinate was fed with a voltage proportional to the magnetic field from a standard resistor. The total X-coordinate error, including the errors of the automatic plotter and of the standard resistor, did not exceed 2%.

The measurements were performed mainly at a temperature of  $2^\circ\text{K}$ . The temperature dependence of the effect was investigated in the interval  $1.9$ – $4.2^\circ\text{K}$ .

### 3. MEASUREMENT RESULTS

In all the investigated cadmium samples in a normal magnetic field we observed oscillations of the quantity  $dR/dH$ , which were approximately periodic in the direct field. The amplitude of the oscillations increased with decreasing temperature. Thus, with decreasing temperature from  $4.2$  to  $2^\circ\text{K}$ , the amplitude increased by a factor 2.8. Therefore all the measurements were carried out at  $T = 2^\circ\text{K}$ .

Sample plots of the oscillations of  $dR/dH$  (as functions of  $H$ ) for different frequencies  $f$  and different sample thicknesses  $d$  are shown in Fig. 2. We see that the oscillations are observed in a magnetic-field interval that is limited from below and from above, and reach a

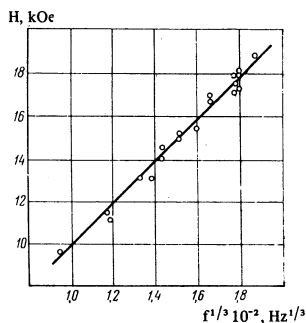


FIG. 3. Frequency dependence of the field  $H_0$  at which the amplitude of the oscillations is maximal.

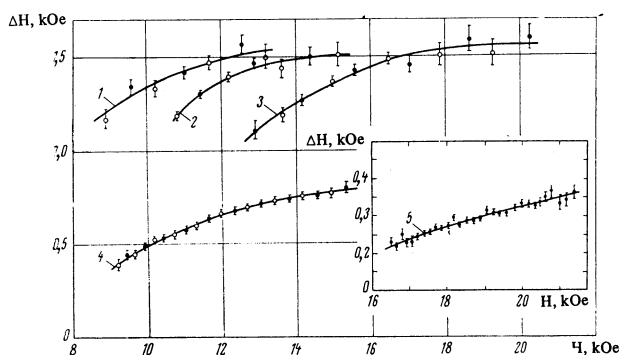


FIG. 4. Dependence of the period of the oscillations  $\Delta H$  on the magnetic field:  $\circ$ —period determined from the maxima of the oscillations of  $dR/dH$ ,  $\bullet$ —period determined from the minima. Curves 1–3 pertain to sample I and correspond to frequencies 0.85, 1.60, and 3.46 MHz; curve 4—sample II, frequency 1.67 MHz; curve 5—sample III, 6.63 MHz. The position of a point on the abscissa axis corresponds to be right-hand extremum of the pair from which the period is determined.

maximum amplitude inside this interval. Some of the plots have quantum oscillations superimposed on the strong-field side. For this reason, a determination of the upper limit of the field interval is difficult in many cases. We see that the amplitude of the long-period oscillations greatly exceeds the amplitude of the quantum oscillations of the impedance. The amplitudes of the oscillations of both types are much larger than the noise of the measuring apparatus.

With increasing frequency, the oscillation picture shifts towards stronger fields. Figure 3 shows a plot of the frequency dependence of the field  $H_0$  at which the amplitude of the oscillations reaches a maximum. We see that with good accuracy  $H_0 \propto f^{1/3}$ . We note that the value of  $H_0$  is practically independent of the thickness of the sample, whereas the positions of the upper and the lower limits of the region of existence of the oscillations come somewhat closer with increasing thickness.

As seen from Fig. 2, the oscillations are not equidistant in the magnetic field; their period increases with increasing  $H$ . Figure 4 shows the dependence of the period of the oscillations  $\Delta H$  on the magnetic field for samples with different thickness. In all cases this dependence has the form of a growing curve with saturation. Curves 1–3, while pertaining to the same sample, correspond to different values of the frequency  $f$ . It should be noted that the asymptotic values of the period

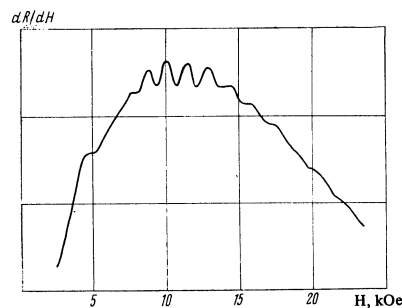


FIG. 5. Sample plot of  $dR/dH$  in a wide interval of magnetic fields;  $T = 2^\circ\text{K}$ ,  $d = 0.4$  mm,  $f = 1.6$  MHz.

in strong fields are quite close for these curves. Curves 4 and 5 pertain to samples of large thickness, and the asymptotic values of the period are smaller for them.

The impedance oscillation amplitude was strongly dependent on the angle  $\theta$  between the normal to the sample and the magnetic field. When  $\theta$  changed from 0 to  $3^\circ$  the amplitude decreased by a factor of two, and at  $\theta = 7^\circ$  it amounted to only 0.2 of the maximum value.

We note that  $dR/dH$  has a large-scale singularity in the field. In most cases the oscillations lie near the top of the large flat maximum of  $dR/dH$ , (see Fig. 5).

4. THEORY

1. The lens model. In metals of the second group with hexagonal lattice, such as magnesium, zinc, and cadmium, there is an electronic Fermi surface in the third zone, in the form of a lens or lentil.<sup>[6]</sup> In the free-electron model it is represented in the form of two spherical segments placed together (see Fig. 6). For cadmium, the radius of the sphere is  $k_F = 1.418 \times 10^8 \text{ cm}^{-1}$ , and the distance from the center of the sphere to the base of the segment is  $k_0 = 1.14 \times 10^8 \text{ cm}^{-1}$ .<sup>[8]</sup> It is convenient to introduce the quantity  $\mu_0 = \cos \vartheta = k_0/k_F = 0.803$ . The volume of the lens is equal to  $k_F^3 V_0$ , where

$$V_0 = \frac{4\pi}{3}(1 - \mu_0)^2 \left(1 + \frac{\mu_0}{2}\right), \tag{1}$$

so that for the electron concentration in the lens  $n_0$  we have

$$n_0 = 2k_F^3 V_0 / (2\pi)^3 = 0.51 \cdot 10^{22} \text{ cm}^{-3} \tag{2}$$

The nonlocal conductivity for a circularly polarized wave propagating along a magnetic field has the following form (see, for example <sup>[9]</sup>, pp. 629 and 630):

$$\sigma_{\pm}^{(e)}(k, \omega) = \pm \sigma_{xy}^{(e)} + i\sigma_{xx}^{(e)} = \frac{e^2}{4\pi^2 \hbar^3} \int dv \frac{m^2(v_F^2 - v_z^2)}{(\mp \Omega - \omega + kv_z - iv)}, \tag{3}$$

where  $\omega$  and  $k$  are the frequency and the wave vector,  $m$  is the effective mass of the electrons,  $v_F = \hbar k_F/m$  is the Fermi velocity,  $v_z$  is the projection of the velocity of the electron on the direction of the magnetic field  $H$  ( $z$  axis),  $\Omega = eH/mc$  is the cyclotron frequency ( $e$  – absolute value of the electron charge), and  $\nu$  is the electron-lattice collision frequency.

Expression (3) for the conductivity is valid in the case of a spherical Fermi surface. In this case the integration with respect to  $v_z$  is carried out from  $-v_F$  to  $v_F$ . The same expression can also be used for the lens model when the magnetic field is parallel to the axis of revolution of the lens. In this case, however, the integration with respect to  $v_z$  should be carried out in two

intervals, from  $-v_F$  to  $-\mu_0 v_F$  and from  $\mu_0 v_F$  to  $v_F$ . Introducing the dimensionless integration variable  $\mu = v_z/v_F$ , we represent expression (3) for the conductivity of the electrons of the lens in the form

$$\sigma_{\pm}^{(e)}(k, \omega) = \mp \frac{n_0 e^2}{m(\Omega \pm \omega \pm i\nu)} \frac{V_q}{V_0}, \tag{4}$$

where

$$V_q = \pi \int_{\mu_1}^1 d\mu \frac{1 - \mu^2}{1 - q\mu} + \pi \int_{-1}^{-\mu_0} d\mu \frac{1 - \mu^2}{1 - q\mu}, \tag{5}$$

$$q = \frac{kv_F}{\Omega \pm \omega \pm i\nu}. \tag{6}$$

The lens volume  $V_0$  defined by (1) is obtained from (5) at  $q = 0$ , so that  $V_{q=0} = V_0$ . Calculation of the integral (5) yields

$$V_q = \frac{2\pi(1 - \mu_0)}{q^2} + \pi \frac{1 - q^2}{q^2} \ln \left( \frac{1 - q}{1 + q} \frac{1 + \mu_0 q}{1 - \mu_0 q} \right). \tag{7}$$

Let us consider the singularities of the nonlocal conductivity  $\sigma_{\pm}^{(e)}(k, \omega)$  in the case of a strong magnetic field, relatively low frequencies, and large mean free paths, when

$$\omega \ll \nu \ll \Omega. \tag{8}$$

Under these conditions, the reduced wave vector  $q$  is almost real ( $q \approx kv_F/\Omega$ ), and the conductivity  $\sigma_{\pm}$  is practically independent of the frequency  $\omega$ . Electrons with  $v_z = v_F$ , traveling along the field  $H$ , are displaced during the cyclotron period by a distance

$$u_0 = 2\pi\nu/v_F. \tag{9}$$

Thus, the quantity  $q$  represents the ratio of the displacement  $u_0$  to the electromagnetic wavelength  $\lambda = 2\pi/k$ .

The nonlocal conductivity defined by formulas (4) and (7) has singularities at  $q = \pm 1$  and  $q = \pm 1/\mu_0$ . The first singularity is due to the Doppler-shifted cyclotron resonance of the electrons of the limiting point, and the second is due to the electrons located in the immediate vicinity of the edge of the lens ( $v_z = \pm \mu_0 v_F$ ). These singularities limit the region of values of the reduced wave vector,  $1 \leq |q| \leq 1/\mu_0$ , within which there exists collisionless cyclotron absorption of the wave by the lens electrons (in this region the argument of the logarithm in formula (7) is negative). It must be borne in mind that the singularity at  $|q| = 1/\mu_0$  is obtained for a lens with an ideally sharp edge. In a real metal the edge of the lens is smoothed out to some degree or another, so that this singularity can shift towards much larger values of  $q$  or may not exist at all. In this case the cyclotron absorption exists in the entire region  $|q| > 1$ . The rounding off of the edge of the lens, however, exerts no influence on the singularity at  $|q| = \pm 1$ , which is due to the electrons of the limiting point.

In the local limit as  $q \rightarrow 0$  the ratio  $V_q/V_0$  tends to unity, and  $\sigma_{\pm}$  coincides with the static Hall conductivity of the lens electrons. Obviously, for the metals of the second group this conductivity is offset by the contribution of the holes. Therefore in such metals the propagation of helicons at  $q \ll 1$  is impossible. To the contrary, when  $q$  is close to unity, the nonlocal conductivity of the lens electrons turns out to be much larger than its local limit. On the other hand, the hole conductivity

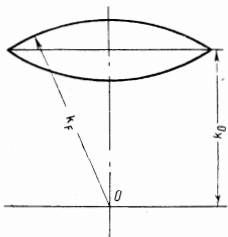


FIG. 6. Cross section of lens in a plane passing through the hexagonal axis.

differs little in this case from its local value, since the displacements of the holes during the cyclotron period are smaller than the displacements of the lens electrons. Therefore when  $q \sim 1$  the cancellation of the electron and hole conductivities is violated. This makes possible the propagation of the doppleron, which is similar to a helicon in the sense that the nonlocal Hall conductivity differs from zero in a certain range of wavelengths. Inasmuch as in this case the electronic conductivity exceeds the hole conductivity, the electromagnetic wave has the same polarization as the helicon, and its properties are determined by the conductivity  $\sigma_-$ .

**2. Properties of the wave.** The dispersion equation determining the spectrum and damping of the wave with negative polarization is given by (see, for example, [9])

$$k^2 c^2 = 4\pi\omega [\sigma_-^{(e)}(k, \omega) + \sigma_-^{(h)}(k, \omega)], \quad (10)$$

where  $\sigma_-^{(e)}$  is the conductivity of the lens electrons, determined by expressions (4)–(7), and  $\sigma_-^{(h)}$  is the conductivity of the hole type, due to all the other carriers. If we neglect the nonlocal effects in  $\sigma_-^{(h)}$ , then its real part should be equal in magnitude and opposite in sign to the local limit  $\text{Re } \sigma_-^{(e)}(k)|_{k \rightarrow 0}$ . Thus, we obtain the following expression for the total conductivity  $\sigma_-$ :

$$\sigma_-(q) = \frac{\pi n_0 e c}{H V_0 (1 - i\gamma)} \left[ \frac{2(1 - \mu_0)}{q^2} + \frac{1 - q^2}{q^3} \ln \left( \frac{1 - q}{1 + q} \frac{1 + \mu_0 q}{1 - \mu_0 q} \right) - \frac{V_0}{\pi} (1 - i\gamma_t) \right], \quad (11)$$

where  $n_0$  and  $V_0$  are given by the formulas (2) and (1).

$$\gamma = v/\Omega, \quad \gamma_t = v_t/\Omega. \quad (12)$$

The term containing  $\gamma_t$  describes the local dissipative conductivity due to the collisions of all the carriers. The quantity  $\gamma_t$  exceeds the quantity  $\gamma$ , since the ratio  $\gamma_t/\gamma$  is proportional to the ratio of the total carrier concentration to the concentration of the lens electrons.

With the aid of (11) it is possible to reduce the dispersion equation (10) to the form

$$\alpha(1 - i\gamma)^3 = \Phi(q), \quad (13)$$

$$\Phi(q) = \frac{1}{2a(1 - a + a^2/3)q^2} \left\{ \frac{2a}{q^2} - 2a^2 \left( 1 - \frac{a}{3} \right) (1 - i\gamma_t) - \frac{1 - q^2}{q^3} \ln \left( \frac{1 - q}{1 + q} \frac{1 - \mu_0 q}{1 + \mu_0 q} \right) \right\}, \quad (14)$$

$$\alpha = \frac{\pi e H^2}{2a(1 - a + a^2/3) c \hbar^2 k_r^2 \omega} = \left( \frac{2\pi\delta}{u_0} \right)^3, \quad (15)$$

where  $a = 1 - \mu_0$  and

$$\delta = \left[ \frac{\pi \hbar c^2}{2a(1 - a + a^2/3) \omega e^2 k_r^2} \right]^{1/2}. \quad (16)$$

The characteristic length  $\delta$  is close in order of magnitude to the thickness of the anomalous skin layer, so that the parameter  $\alpha$  is proportional to the cube of the ratio of this length to the displacement of the limiting-point electrons during the cyclotron period.

We are interested in the solution of the dispersion equation (13) with an almost real value of the wave vector  $k$ . The reduced wave vector

$$q = kv_0 / 2\pi(1 - i\gamma) \quad (17)$$

will also have a small imaginary part. In the limiting case of a very large mean free path, when  $\gamma$  and  $\gamma_t$  tend to zero, the function  $\Phi$  is almost real (at  $|q| < 1$ ) and

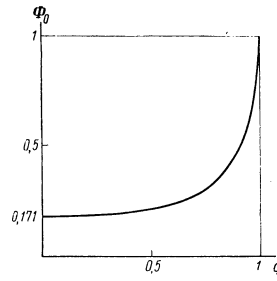


FIG. 7. Plot of the function  $\Phi_0(q')$ .

the solution of the dispersion equation (13) can be sought in the form

$$q = q' + iq'', \quad |q''| \ll |q'| \quad (18)$$

In this approximation, the separation of the real and imaginary parts in (13) can be effected by expanding the function  $\Phi$  in powers of the small quantity  $iq''$ ,

$$\alpha = \Phi_0(q'), \quad (19)$$

$$-3\gamma\alpha = \frac{a(1 - a/3)}{(1 - a + a^2/3)} \frac{\gamma_t}{q'^2} + q'' \frac{d\Phi_0(q')}{dq'}, \quad (20)$$

where the function  $\Phi_0(q')$  differs from  $\Phi(q')$  (14) in the absence of a term proportional to  $\gamma_t$ .

Equation (19) determines the dependence of the real part of  $q'$  on the frequency and on the magnetic field, which enter in the parameter  $\alpha$ , and Eq. (20) makes it possible to determine the imaginary part of  $q$ . By determining  $q$  in this manner and using relation (17), it is easy to find the real and imaginary parts of the wave vector  $k$ .

A plot of the function  $\Phi_0(q')$  is shown in Fig. 7. At  $q' \ll 1$  it tends to a constant limit

$$\Phi_0(0) = \frac{a(1 - 5a/3 + a^2 - a^3/3)}{1 - a + a^2/3}. \quad (21)$$

For the lens dimensions given above, we have  $a = 0.197$ , so that  $\Phi_0(0) = 0.171$ . This limiting value was obtained neglecting nonlocal effects in the conductivity due to the other groups of carriers. Allowance for such effects may change the limiting value and probably decrease it. What is most important for us is that this value is much smaller than unity, as a result of which the region of existence of the wave turns out to be quite wide. As seen from Fig. 7, the effects of spatial dispersion begin to play a role in the region of values of  $q'$  close to unity, where the function  $\Phi_0$  increases rapidly. At  $q' = 1$  it has a termination point, reaching a maximum value of unity. It follows therefore that in the magnetic-field interval corresponding to the variation of the parameter  $\alpha$  from 0.171 to 1 there is a solution of the dispersion equation describing the wave propagation. As is seen from (20), the damping of this wave is inversely proportional to the derivative  $d\Phi_0/dq'$ , so that near the termination point  $q' = 1$ ,  $\alpha = 1$  the damping of the wave turns out to be maximal, increasing rapidly with decreasing magnetic field.

It must be borne in mind that the method described above for solving the complex dispersion equation (13) is not valid near the limiting values of the parameter  $\alpha$ . In the vicinity of the lower limit  $\alpha_{\min} = 0.171$  the derivative  $d\Phi_0/dq'$  vanishes, and at the point  $\alpha_{\max} = 1$  the derivative becomes infinite. Correct allowance for the damping in the region  $\alpha \approx \alpha_{\min}$  causes the minimum

possible value of the reduced wave vector  $q_{\min}$  to be finite:

$$q_{\min} \approx - \left( \frac{1 - a/3}{1 - 3a} \gamma_t \right)^{1/4} e^{-\pi i/8}. \quad (22)$$

For  $\gamma_t = 0.05$ , formula (22) gives for  $q_{\min}$  a value on the order of 0.6. Thus, in the region of existence of the wave the wave vector  $k$  is close to  $2\pi/u_0$ , which is a characteristic property of the doppleron. On the other hand, variation of  $q$  from 0.6 to 1 denotes a noticeable change of the period of the oscillations with changing magnetic field.

The maximum magnetic field  $H_{\max}$  corresponding to the termination point is determined by the condition  $\alpha = 1$ . As the magnetic field approaches  $H_{\max}$  from smaller values, the value of  $q'$  increases and approaches unity. This means that the wave vector  $k$  increases with the magnetic field somewhat more rapidly than linearly. In other words, with increasing magnetic field the wavelength of the doppleron decreases, whereas in the case of the helicon it increases. Therefore the edge of the cyclotron absorption of the helicon lies on the weak-field side, and that of the doppleron on the strong-field side. It should be noted that an experimental measurement of the maximum field  $H_{\max}$  is difficult, since near this edge in cadmium there should exist a Gantmakher-Kaner wave, the length of which is the limiting value of the doppleron wavelength. As shown by an analysis of the excitation conditions, the amplitude of the Gantmakher-Kaner wave is comparable with the amplitude of the doppleron near its termination point. This amplitude is maximal at the point  $H = H_{\max}$ , falling off both in the region of the existence of the doppleron  $H < H_{\max}$ , and in the region of stronger fields  $H > H_{\max}$ . The overlap of the regions of the existence of the doppleron and of the Gantmakher-Kaner wave makes it difficult to determine experimentally the edge of the doppleron  $H_{\max}$ .

3. Excitation of wave in metal and surface impedance. The distribution of the field in a semi-infinite metallic sample is described by the following expression:<sup>[10]</sup>

$$E_-(z) = - \frac{1}{\pi} E_-'(0) \int_{-\infty}^{+\infty} \frac{e^{ikz} dk}{k^2 - 4\pi\omega c^{-2}\sigma_-(k)}, \quad (23)$$

where  $E_-'(0)$  is the derivative of the electric field with respect to the normal on the surface of the metal  $z = 0$ . Expression (23) was obtained for specular reflection of the electrons from the surface of the metal. The same formula will be valid also for the distribution of the field in a plate whose thickness greatly exceeds the damping length of the electromagnetic wave in the

metal, if the wave is excited on one side of the plate. On the other hand, if the plate is placed inside a coil and two-sided antisymmetrical (with respect to the electric field) excitation of the wave takes place, then it is necessary to subtract from the right-hand side of (23) a similar expression, in which the coordinate  $z$  is replaced by  $d - z$ . This term describes the part of the field due to the excitation from the opposite side of the plate. As a result the surface impedance of a thick plate can be represented in the form

$$Z_- = - 8i\omega \int_{-\infty}^{+\infty} dk \frac{1 - e^{ikd}}{k^2 c^2 - 4\pi\omega\sigma_-(k)}, \quad (24)$$

where  $d$  is the thickness of the plate. The term with unity in the numerator of the integrand describes the impedance of a semi-infinite metal, which at  $\omega \ll \nu$  has a smooth dependence on the magnetic field. This term has little influence on the oscillating part of the impedance, and we shall not consider it here. The term containing the factor  $e^{ikd}$  is a rapidly oscillating function of  $H$  and is our main interest.

Denoting this part of the impedance by  $\Delta Z_-$  and changing over from integration with respect to  $k$  to integration with respect to  $q$ , we write it in the form

$$\Delta Z_- = \frac{8i\omega\delta}{c^2} \alpha^{2/3} (1 - i\gamma)^2 \int_C \frac{dq}{q^2} \frac{\exp[q(d/l + 2i\pi d/u_0)]}{\alpha(1 - i\gamma)^3 - \Phi(q)}, \quad (25)$$

where  $l = v_F/\nu$  is the mean free path of the lens electrons. The integration contour  $C$  (see Fig. 8) constitutes a straight line inclined to the real axis at an angle  $\gamma$ . To calculate the integral, we close the contour of integration in the upper half-plane in the manner shown by the dashed line. The contour goes around the pole  $p$  of the integrand in the upper half-plane and the edge of the cut between the two branch points  $q_1 = -1$  and  $q_2 = -1/\mu_0$ . The residue at the pole,  $\Delta Z_-^{(p)}$ , constitutes the impedance due to excitation of the doppleron in the plate, while the integral over the edges of the cut  $Z_-^{(GK)}$  describes the radio-frequency size effect (the Gantmakher-Kaner wave<sup>[7]</sup>). Thus, the impedance of the plate takes the form

$$\Delta Z_- = \Delta Z_-^{(p)} + Z_-^{(GK)}, \quad (26)$$

where

$$\Delta Z_-^{(p)} = \frac{4\pi\omega\delta}{c^2} A(q_0) \exp \left[ -\kappa(q_0)d + iq_0' \frac{2\pi d}{u_0} \right], \quad (27)$$

$$A(q_0) = 4(1 - i\gamma)^2 \alpha^{2/3} \left\{ \frac{d}{dq} [q^2 \Phi(q) - q^2 u] \right\}_{q=q_0}^{-1}, \quad (28)$$

$$\kappa(q_0) = - \frac{q_0'}{l} + \frac{2\pi}{u_0} q_0''. \quad (29)$$

The pole  $q = q_0 \equiv q_0' + iq_0''$  lies in the second quadrant near the branch point  $q_1 = -1$ . The amplitude  $A(q_0)$  is inversely proportional to the derivative  $d\Phi/dq$ . Therefore,  $A(q_0)$  tends to zero at the point of termination of the doppleron as  $\alpha \rightarrow 1$ , and increases in the region of weak fields as  $\alpha \rightarrow \alpha_{\min}$ . The damping of the wave  $\kappa(q_0)$ , to the contrary, is small in the region of strong fields and large near  $\alpha = \alpha_{\min}$ . Therefore the impedance (27) has a maximum inside the interval between  $\alpha_{\min}$  and  $\alpha_{\max}$ .

The period of the oscillations is determined by the phase of the impedance (27), which depends on the mag-

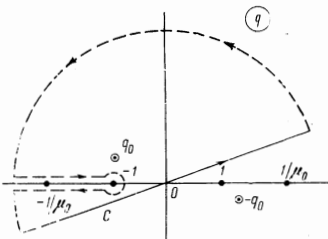


FIG. 8. Integration contour in the complex  $q$  plane.

netic field. The thickness of the plate  $d$  subtends a large number of displacements  $u_0$ , as a result of which this phase is quite large and the impedance (27) is a rapidly oscillating function of the magnetic field. The period of the oscillations  $\Delta H$  corresponds to a change of the phase by  $2\pi$  and can be determined from the condition

$$2\pi = -\frac{d}{dH} \left( \frac{2\pi d}{u_0} q_0' \right) \Delta H, \quad (30)$$

From this we get

$$\Delta H = (\Delta H)_{GK} \left| q_0' + H \frac{dq_0'}{dH} \right|^{-1}, \quad (31)$$

where

$$(\Delta H)_{GK} = 2\pi \hbar k_F c / ed \quad (32)$$

is the period of the Gantmakher-Kaner oscillations.<sup>[7]</sup>

At magnetic-field values not too close to  $H_{\min}$  and  $H_{\max}$ , formula (31) for the conversion of the oscillations can be expressed in terms of the function  $\Phi_0$ :

$$\Delta H = \frac{(\Delta H)_{GK}}{|q' + 3\Phi_0(d\Phi_0/dq')^{-1}|}. \quad (33)$$

The functions  $q'$ ,  $\Phi_0$ , and  $d\Phi_0/dq'$  increase monotonically with increasing magnetic field from  $H_{\min}$  to  $H_{\max}$ . The derivative  $d\Phi_0/dq'$  increases most rapidly here, so that as a result the denominator of the right-hand side of (33) decreases with increasing field, approaching unity as  $H \rightarrow H_{\max}$ . In other words, the period of the oscillations  $\Delta H$  increases monotonically with the magnetic field and near the termination point  $H_{\max}$  it reaches its limiting value, equal to  $(\Delta H)^{GK}$ .

At magnetic-field values close to  $H_{\min}$ , the  $q_0'(H)$  dependence can be obtained by expanding the function  $\Phi(q)$  in powers of  $q^2$ :

$$\Phi(q) \approx \alpha_{\min} + \alpha_2 q^2 + i\gamma_t \frac{a(1-a/3)}{1-a+a^2/3}, \quad (34)$$

where

$$\alpha_2 = \frac{a(1-3a+4a^2)}{1-a+a^2/3} = 0.138,$$

and  $\alpha_{\min}$  is determined by formula (21). Substituting (34) in the dispersion equation (13) and solving the resultant equation for  $q$ , we obtain the position of the pole:

$$q_0 \approx - \left[ \frac{\gamma_t \left(1 - \frac{a}{3}\right)}{1 - 3a + 4a^2} \right]^{1/2} e^{-i\pi/8} \left\{ 1 + \frac{\alpha_{\min}}{4\alpha_2} \left[ \frac{1 - 3a + 4a^2}{\gamma_t (1 - a/3)} \right]^{1/2} e^{i\pi/4} \right\} \quad (35)$$

Calculating the derivative  $dq_0'/dH$ , we can obtain the following expression for the period of the oscillations near the lower edge:

$$\Delta H_{\min} = \frac{4}{3|q_{\min}'|} \left\{ 1 + \frac{\alpha_{\min}}{\alpha_2} \left[ \frac{1 - 3a + 4a^2}{\gamma_t (1 - a/3)} \right]^{1/2} \right\}^{-1} (\Delta H)_{GK}, \quad (36)$$

where  $q_{\min}'$  is the value of  $q_0'$  at  $\alpha = \alpha_{\min}$  (see also formula (22)).

Let us stop to discuss briefly the term  $Z^{(GK)}$ , which is connected with the quasistationary electromagnetic field and is described by the integral over the edges of the cut. The main contribution to this integral is made by a small vicinity of the branch point  $q = -1$ . Consequently  $Z^{(GK)}$  contains an oscillating exponential  $\exp(-i2\pi d/u_0)$ , which gives Gantmakher-Kaner oscilla-

tions that are equidistant in the direct field. Calculation shows that inside the region of existence of the doppleron ( $\alpha < 1$ ) the amplitude of the oscillations of  $Z^{(GK)}$  is small compared with the amplitude of the doppleron. In the vicinity of the upper edge of the doppleron ( $\alpha \approx 1$ ) the impedance  $Z^{(GK)}$  has a maximum, the value of which is of the same order as the amplitude of the doppleron in this region. Therefore when  $\alpha \approx 1$  the Gantmakher-Kaner oscillations are practically indistinguishable from the doppleron. In the region of strong fields ( $\alpha > 1$ ) there exist only the Gantmakher-Kaner oscillations, the amplitude of which decreases in the region  $\alpha \gtrsim 1$  and then tends to a constant limit proportional to  $(\delta/d)^2 \exp(-d/l)$ .

## 5. DISCUSSION OF RESULTS

A comparison of the experimental results with the conclusions of the theory allow us to state that the observed oscillations of the surface impedance of cadmium are connected with excitation in the sample of propagating electromagnetic waves—dopplérons. The characteristic properties of dopplérons are the presence of upper and lower limits of the region of existence of the wave  $H_{\min}$  and  $H_{\max}$ , and the dependence of the period of the oscillations on the magnetic field. In weak magnetic fields, the period of the oscillations is relatively small and increases with increasing field, reaching a maximum value near the upper limit of existence of the wave. According to the conclusions of the theory, this limiting value should coincide with the period of the oscillations of the radio-frequency size effect. A similar change of the period with changing magnetic field was observed experimentally (Fig. 4). The limiting value of the period  $\Delta H_l$  for a sample 0.40 mm thick (curves 1–3) is  $1540 \pm 80$  Oe, and for a sample 0.76 mm thick it is equal to  $800 \pm 40$  Oe. Formula (32) for the limiting value of the period can be written in the form

$$(\Delta H)_{GK} = 41.2 k_F / d, \quad (32a)$$

where  $k_F$  is the radius of curvature of the lens at the limiting point in  $\text{\AA}^{-1}$ ,  $d$  is the thickness in centimeters, and  $(\Delta H)^{GK}$  is the period of the oscillations in oersteds. We then obtain from formula (32a) and from the presented data

$$k_F = 1.49 \pm 0.08 \text{\AA}^{-1}.$$

The obtained value of the radius of curvature can be regarded as in agreement (within the limits of measurement accuracy) with the value  $k_F = 1.42 \text{\AA}^{-1}$  given by the free-electron model.<sup>[8]</sup> The radius of curvature  $k_F = 1.3 \pm 0.1 \text{\AA}^{-1}$  obtained in<sup>[11]</sup> is somewhat smaller than the value measured by us.

As seen from Fig. 4, the total change of the period, referred to the period of the Gantmakher-Kaner oscillations, amounts to 30–50%. Theoretically this quantity can be calculated from formula (36). The minimum values of the reduced wave vector  $q_{\min}$  and of the period of the oscillations  $\Delta H_{\min}$  are determined by the effective dimensionless collision frequency  $\gamma_t$ . The value of  $\gamma_t$  can be determined from data on the magnetoresistance of cadmium. It follows from the results of<sup>[12]</sup> that  $\gamma_t \approx 0.01$  in a field  $H = 15$  kOe at a resistance

Sample No.	d, mm	f, MHz	H <sub>min</sub> , kOe	H <sub>max</sub> , kOe	H <sub>min</sub> f <sup>-1/3</sup> , kOe-MHz <sup>-1/3</sup>	H <sub>max</sub> f <sup>-1/3</sup> , kOe-MHz <sup>-1/3</sup>
I	0.40	0.85	7	13	7.4	13.8
I	0.40	1.60	8.5	16	7.3	13.7
I	0.40	3.46	11	21	7.3	13.9
II	0.76	1.67	8.5	17	7.2	14.3
II	0.76	2.65	10	19	7.2	13.8
II	0.76	4.06	12	21,5	7.6	13.5
III	1.46	4.56	13.5	21	8.2	12.7
III	1.46	4.6	13	21	7.8	12.6
III	1.46	5.70	14	23	7.8	12.8
III	1.46	6.63	15	23	8.0	12.3
IV	1.48	2.90	11	18,5	7.7	13.0
IV	1.48	5.63	12	22	7.9	12.4
V	1.48	2.90	12	18	8.8	12.7
V	1.48	3.47	13	19	8.6	12.6

ratio  $\rho(300^\circ\text{K})/\rho(4.2^\circ\text{K}) = 4 \times 10^4$ . For the samples used in our investigation, the ratio of the resistances is approximately  $1 \times 10^4$ , so that at  $H = 9$  kOe the value of  $\gamma_t$  is 0.067. For this value of  $\gamma_t$ , the period of the oscillations  $\Delta H_{\text{min}}$ , calculated from formula (36), is  $0.51 (\Delta H)_{\text{GK}}$ . Thus, the relative change of the period is 49%, in agreement with the experimental results.

Let us stop now and discuss the position of the upper and lower limits of the region of existence of the doppleron. The position of the upper limit,  $H_{\text{max}}$ , is determined by the condition  $\alpha = 1$  and is given by the formula

$$H_{\text{max}} = 14[a(1 - a + a^2/3)k_F^2 f]^{1/3}, \quad (37)$$

which follows from (15). Here  $k_F$  is measured in  $\text{\AA}^{-1}$ , the frequency  $f$  in MHz, and  $H_{\text{max}}$  in kOe. Substituting the values  $k_F = 1.42 \text{\AA}^{-1}$  and  $a = 0.197$  corresponding to the model of almost free electrons, we obtain

$$H_{\text{max}} = 13.6f^{1/3}. \quad (38)$$

The position of the lower limit  $H_{\text{min}}$  is determined by the condition  $\alpha = \alpha_{\text{min}} = 0.17$ , from which it follows that

$$H_{\text{min}} = \alpha_{\text{min}}^{1/3} H_{\text{max}} = 7.5f^{1/3}. \quad (39)$$

The table lists the values of the fields  $H_{\text{min}}$  and  $H_{\text{max}}$  measured for five samples in the frequency interval 0.85–6.63 MHz. The lower limiting field  $H_{\text{min}}$  was determined from the appearance of the oscillations. In Fig. 2, these values are marked by an arrow. The determination of the upper limiting field  $H_{\text{max}}$  is made difficult by the distortions of the  $dR/dH$  curves by the quantum oscillations, and also by the presence of the Gantmakher-Kaner radio-frequency size effect oscillations, the amplitude of which decreases slowly with the field. Allowance for the latter circumstance is particularly important for thin samples, on which the Gantmakher-Kaner effect is clearly seen in strong fields. Therefore in the determination of  $H_{\text{max}}$  for these samples we took into account two attributes of the Gantmakher-Kaner oscillations: the constancy of the period, and the weak dependence of the amplitude on the field. The doppleron oscillations, to the contrary, are characterized by dispersion of the period and by a rapid decrease of the amplitude near the edge. These singularities can be illustrated by the saturation of the period of the oscillations in Fig. 3 and by the slow change of the amplitude of the oscillations on curve 3 of Fig. 2, starting with a field  $H \approx 17$  kOe. Guiding ourselves by these attributes, we determined the position of the upper limit of the doppleron  $H_{\text{max}}$ . On the curves

2 and 3 of Fig. 2, these fields are marked by arrows. For thick samples, the position of  $H_{\text{max}}$  was determined simply as the field at which the long-period oscillations characteristic of the doppleron vanish.

For convenience in comparison of the experimental values of the limits with formulas (38) and (39), the table also lists the values of the reduced fields  $H_{\text{min}}f^{-1/3}$  and  $H_{\text{max}}f^{-1/3}$ . According to formula (37), these quantities are determined only by the dimensions of the lens and should not depend on the frequency and on the sample thickness. For the free-electron model (see (38) and (39)), the reduced fields are equal to approximately 7.5 and 13.6 kOe-MHz<sup>-1/3</sup>. For thin samples I and II, the minimum reduced field ranges from 7.2 to 7.6, and the maximum from 13.5 to 14.3. Thus, the positions of both the lower and the upper limits are in good agreement with the theoretical values. For the thick samples III–V the agreement is poorer: the position of the lower limit varies in the range 7.8–8.8, and that of the upper changes from 12.3 to 13. In other words, the region in which the doppleron oscillations are observed becomes narrower, and its limits shift towards the center. This is natural, since near the limits the amplitude of the wave is small and in thick samples the wave does not reach the opposite side of the plate.

The constancy of the reduced limiting fields denotes that, in accordance with the theory,  $H_{\text{min}}$  and  $H_{\text{max}}$  are proportional to  $\omega^{1/3}$ . The field  $H_0$  at which the amplitude of the oscillations is maximal should also be proportional to  $\omega^{1/3}$ , but the proportionality coefficient should depend on the ratio of the thickness of the sample to the mean free path of the lens electrons. Nonetheless, the values of  $H_0$  for all the samples shown in Fig. 3 practically fit one straight line. This may be connected either with the weak dependence of  $H_0$  on  $d/l$  or with the small variation of the ratio  $d/l$  for our samples.

As already noted above, quantum oscillations of the impedance are observed in strong fields. Their amplitude is modulated at the frequency of the Gantmakher-Kaner oscillations. This modulation is particularly clearly seen on curve 3 of Fig. 2. This indicates that the quantum are connected with the transmitted wave.

The foregoing comparison of the theoretical and experimental results shows that the observed long-period oscillations of the impedance of the plates of cadmium are due to excitation of a doppleron. In this connection we note that oscillations of similar type, recalling the radio-frequency size effect, were observed in copper<sup>[13-15]</sup> and in indium.<sup>[16]</sup> It is possible that these oscillations are also connected with excitation of a doppleron (see<sup>[15]</sup>).

The authors are grateful to Professor V. G. Fastovskii for constant interest in the work, to I. P. Krylov for useful discussions and valuable advice, to A. V. Gavrilov for technical help, and to N. B. Brovtsyna for numerical calculations.

<sup>1</sup>R. G. Chambers and V. G. Skobov, J. Phys., in press.

<sup>2</sup>D. S. Falk, B. Gerson, and J. F. Carolan, Phys. Rev. B1, 407 (1970).

<sup>3</sup>J. C. McGroddy, J. R. Stanford, and E. A. Stern, Phys. Rev. 141, 437 (1966).

- <sup>4</sup>A. W. Overhauser and S. Rodriguez, *Phys. Rev.* **141**, 246 (1966).
- <sup>5</sup>O. V. Konstantinov and V. G. Skobov, *Fiz. Tverd. Tela* **12**, 2768 (1970) [*Sov. Phys.-Solid State* **12**, 2237 (1971)].
- <sup>6</sup>D. Shoenberg, In *The Physics of Metals 1, Electrons*, ed. by J. Ziman, Cambridge University Press, p. 104.
- <sup>7</sup>V. F. Gantmakher and É. A. Kaner, *Zh. Eksp. Teor. Fiz.* **48**, 1572 (1965) [*Sov. Phys.-JETP* **21**, 1053 (1965)].
- <sup>8</sup>M. P. Shaw, T. G. Eck, and D. A. Zych, *Phys. Rev.* **142**, 406 (1966).
- <sup>9</sup>E. A. Kaner and V. G. Skobov, *Adv. in Phys.* **17**, 605 (1968).
- <sup>10</sup>G. E. Reuter and E. H. Sondheimer, *Proc. Roy. Soc. A* **195**, 336 (1948).
- <sup>11</sup>V. P. Naberezhnykh and A. A. Maryakhin, *Phys. Stat. Sol.* **20**, 737 (1967).
- <sup>12</sup>O. P. Katyal and A. N. Gerritsen, *Phys. Rev.* **178**, 1037 (1969).
- <sup>13</sup>G. Weisbuch and A. Libchaber, *Phys. Rev. Lett.* **19**, 498 (1967).
- <sup>14</sup>B. Perrin, G. Weisbuch, and A. Libchaber, *Phys. Rev.* **B1**, 1501 (1970).
- <sup>15</sup>P. A. Antoniewicz, L. T. Wood, and J. D. Gavenda, *Phys. Rev. Lett.* **21**, 998 (1968).
- <sup>16</sup>I. P. Krylov, *Zh. Eksp. Teor. Fiz.* **54**, 1738 (1968) [*Sov. Phys.-JETP* **27**, 934 (1968)].

Translated by J. G. Adashko  
82